The Journal of Chemical Physics ARTICLE scitation.org/journal/jcp

Polymer escape through a three dimensional double-nanopore system

Cite as: J. Chem. Phys. 153, 104901 (2020); doi: 10.1063/5.0015310
Submitted: 15 June 2020 • Accepted: 23 August 2020 •
Published Online: 10 September 2020

View Online Export Citation CrossMark

Swarnadeep Seth and Aniket Bhattacharya[a)]

AFFILIATIONS

Department of Physics, University of Central Florida, Orlando, Florida 32816-2385, USA

[a)]Author to whom the correspondence should be addressed: AniketBhattacharya@ucf.edu

ABSTRACT

We study the escape dynamics of a double-stranded DNA (dsDNA) through an idealized double nanopore geometry subject to two equal and opposite forces (tug-of-war) using Brownian dynamics (BD) simulation. In addition to the geometrical restrictions imposed on the cocaptured dsDNA segment in between the pores, the presence of tug-of-war forces at each pore results in a variation of the local chain stiffness for the segment of the chain in between the pores, which increases the overall stiffness of the chain. We use the BD simulation results to understand how the intrinsic chain stiffness and the tug-of-war forces affect the escape dynamics by monitoring the local chain persistence length ℓ_p, the residence time of the individual monomers $W(m)$ in the nanopores, and the chain length dependence of the escape time $\langle\tau\rangle$ and its distribution. Finally, we generalize the scaling theory for the unbiased single nanopore translocation for a fully flexible chain for the escape of a semi-flexible chain through a double nanopore in the presence of tug-of-war forces. We establish that the stiffness dependent part of the escape time is approximately independent of the translocation mechanism so that $\langle\tau\rangle \sim \ell_p^{2/D+2}$, and therefore, the generalized escape time for a semi-flexible chain can be written as $\langle\tau\rangle = AN^{\alpha}\ell_p^{2/D+2}$. We use the BD simulation results to compare the predictions of the scaling theory. Our numerical studies supplemented by scaling analysis provide fundamental insights to design new experiments where a dsDNA moves slowly through a series of graphene nanopores.

Published under license by AIP Publishing. https://doi.org/10.1063/5.0015310

I. INTRODUCTION

Recently, mechanical trapping of DNA in a double nanopore platform has been demonstrated to be a more effective alternative for analyzing DNA sequences and offers new opportunities for DNA manipulation.[1] Compared to the original design of single nanopore and nanochannel based techniques,[2–5] in a double nanopore system, a DNA is electrophoretically captured in two nanopores, which are drilled in parallel through the same solid-state membrane. It has been demonstrated that trapping increases the residence time by an order of magnitude, providing ample time to analyze the cocaptured segment in between the pores more accurately.[1] Different variations of this concept, such as two pores of different width,[1] double nanopore separated by a nano-bridge,[6] and double-barrel nanopore (NP),[7] have been reported. Compared to a single nanopore device, the adjustable biases and feedback mechanism at each pore offer overall better control of the DNA and allow us to achieve a force balanced tug-of-war situation.[8] This idea of the mechanical arrest of a translocating DNA into a solid-state double nanopore platform[1] has been further exploited in more recent experiments where an alternating net differential bias on two nanopores allow the electrophoretically captured DNA to oscillate back and forth from one reservoir to the other, enabling a specific DNA segment to be analyzed multiple times by keeping the DNA captured at all-time in both the pores. These multiple scans of several hundred times increase the accuracy of this method significantly so that the method has a potential application for determining DNA barcodes.[9,10]

While translocation through a single nanopore system has been studied quite extensively theoretically, experimentally, and using a variety of numerical and simulation strategies,[11] theoretical studies and modeling translocation in double or multiple NP system are only just the beginning.[1,12] In Ref. 1, the persistence length of the DNA and the time scale of the electrophoretic mobility were used to obtain the parameters of the coarse-grained model used in the molecular dynamics (MD) simulation studies to explain the

Published under license by AIP Publishing

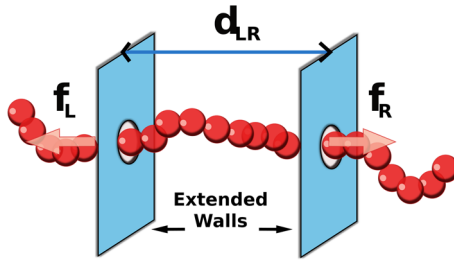

FIG. 1. Schematics of a chain of contour length L, where σ is the diameter of the individual monomers cocaptured by the two nanopores separated by distance d_{LR}. The two walls extend in yz plane, and external biases $\vec{f}_L = -|f_L|\hat{x}$ and $\vec{f}_R = |f_R|\hat{x}$ along negative and positive x directions, respectively, are applied inside each pore of equal diameters $d_{pore} = 2\sigma$.

experimental results in terms of simulation parameters, while in Ref. 12, several aspects of an ideal two-dimensional double nanopore system were studied in a more general framework. In this letter, we report Brownian dynamics (BD) simulation studies of a homopolymer escape through a double nanopore (DNP) system. The design of our ideal double nanopore system *in silico* (Fig. 1) has been motivated by recent experiments where the nanopores are drilled onto a single wafer as reported recently,[1,9,10] but our geometry resembles a multilayered graphene nanopore, where first principles transport calculations for DNA bases surveyed across a graphene nanopore system have illustrated the advantages of this geometry.[13] Thus, it is conceivable that future experiments will be carried out in this geometry of parallelly stacked graphene nanopores. Another purpose of choosing this geometry is that in the limit $d_{LR}/L \ll 1$, it is expected that some characteristics of the double nanopore translocation will show similarities with the corresponding quantities in the single nanopore translocation and can be analyzed using the known theoretical and simulation studies of single nanopore translocation.[11] We expect that these studies will also provide information to design new experiments with different parameter sets as well as will provide insights to develop a theoretical framework of double multi-pore translocation for different geometries.

II. MODEL

Our BD scheme is implemented on a bead-spring model of a polymer with the monomers interacting via an excluded volume (EV), a Finite Extension Nonlinear Elastic (FENE) spring potential, and a bond-bending potential enabling variation of the chain persistence length ℓ_p (Fig. 1). The model, originally introduced for a fully flexible chain by Grest and Kremer,[14] has been studied quite extensively by many groups using both Monte Carlo (MC) and various molecular dynamics (MD) methods.[15] Recently, we have generalized the model for a semi-flexible chain and studied both equilibrium and dynamic properties.[16,17] Comparison of our BD results with those obtained for very large self-avoiding chains on a square lattice reveals robustness of the model for certain universal aspects, e.g., scaling of the end-to-end distance and transverse fluctuations.[17,18] Using our BD scheme for confined stiff polymers in nanochannels, we have demonstrated and verified the existence of Odijk deflection length $\lambda \sim (\ell_p D^2)^{1/3}$.[18] Last but not the least, we have used the same model earlier to address various problems in single nanopore translocation with success.[19,21] The successes of these prior studies explaining a variety of phenomena assure that the BD simulation studies will provide useful information and insights toward a fundamental understanding of polymer translocation through a model double nanopore system.

The EV interaction between any two monomers is given by a short range Lennard-Jones (LJ) potential

$$U_{\rm LJ}(r) = 4\epsilon\left[\left(\frac{\sigma}{r}\right)^{12} - \left(\frac{\sigma}{r}\right)^{6}\right] + \epsilon \text{ for } r \le 2^{1/6}\sigma;$$
$$= 0, \text{ for } r > 2^{1/6}\sigma. \quad (1)$$

Here, σ is the effective diameter of a monomer, and ϵ is the strength of the LJ potential. The connectivity between neighboring monomers is modeled as a FENE spring with

$$U_{\rm FENE}(r_{ij}) = -\frac{1}{2}k_F R_0^2 \ln\left(1 - r_{ij}^2/R_0^2\right). \quad (2)$$

Here, $r_{ij} = |\vec{r}_i - \vec{r}_j|$ is the distance between the consecutive monomer beads i and $j = i \pm 1$ at $\vec{r}_i$ and $\vec{r}_j$, k_F is the spring constant, and R_0 is the maximum allowed separation between connected monomers. The chain stiffness κ is introduced by adding an angle dependent three-body interaction term between successive bonds as (Fig. 1)

$$U_{\rm bend}(\theta_i) = \kappa(1 - \cos\theta_i). \quad (3)$$

Here, θ_i is the angle between the bond vectors $\vec{b}_{i-1} = \vec{r}_i - \vec{r}_{i-1}$ and $\vec{b}_i = \vec{r}_{i+1} - \vec{r}_i$, respectively, as shown in Fig. 1. The strength of the interaction is characterized by the bending rigidity κ associated with the ith angle θ_i. For a homopolymer chain, the bulk persistence length ℓ_p of the chain in three dimensions (3D) is given by[22]

$$\ell_p/\sigma = \kappa/k_B T. \quad (4)$$

Each of the two purely repulsive walls consists of one monolayer (line) of immobile LJ particles of the same diameter σ of the polymer beads symmetrically placed at $\pm\frac{1}{2}d_{LR}$. The two nanopores are created by removing particles at the center of each wall (Fig. 1). We use the Langevin dynamics with the following equations of motion for the ith monomer,

$$m\ddot{\vec{r}}_i = -\nabla\left(U_{\rm LJ} + U_{\rm FENE} + U_{\rm bend} + U_{\rm wall}\right) - \Gamma\vec{v}_i + \vec{\eta}_i. \quad (5)$$

Here, $\vec{\eta}_i(t)$ is a Gaussian white noise with zero mean at temperature T and satisfies the fluctuation–dissipation relation in d physical dimensions (here $d = 3$),

$$\langle\vec{\eta}_i(t)\cdot\vec{\eta}_j(t')\rangle = 2dk_B T\Gamma\,\delta_{ij}\,\delta(t - t'). \quad (6)$$

We express length and energy in units of σ and ϵ, respectively. The parameters for the FENE potential in Eq. (2), k_F and R_0, are set to $k_F = 30\epsilon/\sigma$ and $R_0 = 1.5\sigma$, respectively. The friction coefficient and the temperature are set to $\Gamma = 0.7\sqrt{m\epsilon/\sigma^2}$ and $k_B T/\epsilon = 1.2$, respectively. The force is measured in units of $k_B T/\sigma$.

Published under license by AIP Publishing

The numerical integration of Eq. (5) is implemented using the algorithm introduced by van Gunsteren and Berendsen.[23] Our previous experiences with BD simulation suggests that for a time step $\Delta t = 0.01$, these parameters values produce stable trajectories over a very long period of time and do not lead to unphysical crossing of a bond by a monomer.[17,18] The average bond length stabilizes at $b_l = 0.971 \pm 0.001$ with negligible fluctuation regardless of the chain size and rigidity.[17] We have used a Verlet neighbor list[24] instead of a link-cell list to expedite the computation.

III. RESULTS

The starting conformation of our BD simulation is a DNA polymer already captured and threaded through both the pores as in Fig. 1. We symmetrically place the polymer in a double nanopore device and equilibrate the polymer chain keeping two polymer beads inside each pore clamped. We equilibrate the polymer over 10 times the Rouse relaxation time $\tau_{Rouse} \sim N^{1+2\nu}$, where $\nu = 0.588$ is the Flory exponent in 3D (for N = 128, this corresponds to 10^8 time steps);[25] the polymer chain is allowed to translocate under the influence of two external forces $\vec{f}_L$ and $\vec{f}_R$. In this paper, we only consider the tug-of-war situation $\vec{f}_L + \vec{f}_R = 0$ so that the polymer chain diffuses across the entropic barrier imposed by the pores. To calculate relevant physical quantities, we take average over 2000 successful translocation events for several chain lengths $L = 128\sigma$–256σ and for several values of stiffness parameter $\kappa = 0$–128.

The order of the following subsections (Secs. III A–III C) are as follows: Since a major difference of the double nanopore translocation in a tug-of-war situation, when compared to an unbiased translocation through a single nanopore, that is, the chain segment in between the two pores is under tension, we first provide a detail picture of the evolving chain persistence length during translocation (Sec. III A). This helps to understand the shape of the dwell time distribution presented next (Sec. III B). It is worth mentioning that the dwell time (or often it is called the residence time) is directly correlated with the current blockade time in an experiment. One of the goals of these double nanopore experiments is to maintain the segment in between the pores in a straight conformation. We have monitored the transverse fluctuation of the chain in between the pores to check the chain conformation in between the pores (Sec. III B). Finally, we present the results for the escape of chain making a comparison with those for the unbiased single nanopore translocation (Sec. III C).

A. Chain persistence length during translocation

The instantaneous chain stiffness $\ell_p(m)$ as a function of the monomer index m calculated from

$$\ell_p(m) = -\frac{1}{\ln[\cos(\theta_m)]}, \tag{7}$$

where θ_m is the angle subtended by the adjacent bond vectors connecting the monomer m,[25] is shown Fig. 2(a) at different times, which shows that the chain segment acquires an increased stiffness while crossing the region in between the two pores. As time progresses, the position of the maxima does not necessarily occur at the increasing value of the reduced monomer index m/N due to the back and forth motion of the chain. The corresponding time averaged stiffness is shown in Fig. 2(b), which shows that the relative increase in the persistence length $\ell_p/\langle\ell_p\rangle$ is most significant for $\kappa = 0$. The chain segment in between the pores experiences equal and opposite forces, which further increases the stiffness by restricting the entropic penalty. This reduction is entropy is less significant for a stiffer chain, which explains the effect. This effect will be important if the experiments were done with the single stranded DNA. Figure 2 has implication in the corresponding dwell time distribution, as discussed next.

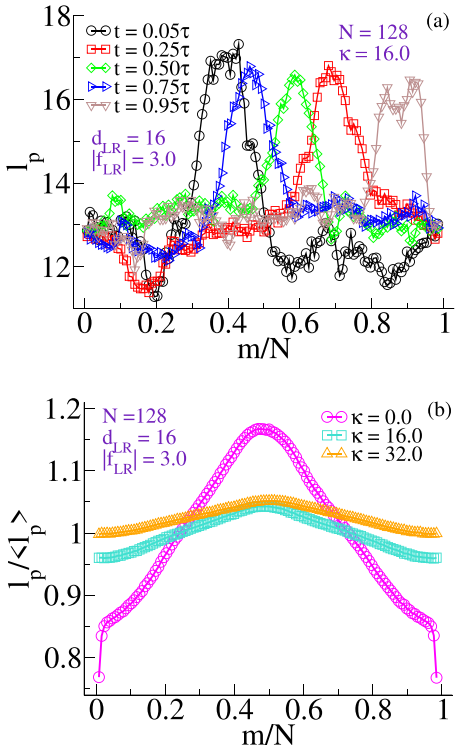

FIG. 2. (a) The instantaneous local chain persistence length $\ell_p(m)$ at five different instances: $t = 0.05\tau$ (black circles), $t = 0.25\tau$ (red squares), $t = 0.50\tau$ (green diamonds), $t = 0.75\tau$ (blue triangles), and $t = 0.95\tau$ (brown down triangles) showing that different parts of the chain become stiffer at different times of the translocation process. (b) Normalized time averaged persistence length $l_p/\langle\ell_p\rangle$ as a function of reduced monomer index m/N for $\kappa = 0$ (magenta circles), $\kappa = 16$ (teal squares), and $\kappa = 32$ (orange triangles), respectively. The relative increase in ℓ_p is most prominent for $\kappa = 0$.

B. The dwell time distribution

Extracting dwell time distribution from the simulation data as a function of the monomer index is a key quantity as it mimics the current blockade data in a nanopore experiment. The normalized $\tilde{W}(m)$ is defined as

$$\langle\tilde{W}(m)\rangle = \frac{1}{\sum_{m=1}^{N} W(m)}\langle W(m)\rangle. \tag{8}$$

Published under license by AIP Publishing

By definition, $\sum_{m=1}^{N} W(m) = \tau$, where τ is the escape time; hence, $\sum_{m=1}^{N} \tilde{W}(m) = 1$. Thus, $\tilde{W}(m)$ provides the relative time spent by the individual monomer during the translocation process, as shown in Fig. 3. The quantity has been calculated for the unbiased single nanopore translocation and shares qualitatively similar features[36] excepting minor modification in its shape near $N/2 - \frac{1}{2}d_{LR}/\sigma < m < N/2 + \frac{1}{2}d_{LR}/\sigma$ due to the presence of two pores. For the unbiased translocation in a single nanopore, $W(m)$ is symmetric and peaks at $m = N/2$, simply due to the fact the entropic force is balanced at either side of the pore, as has been observed previously.[36] For the escape problem in a double nanopore in a tug-of-war situation, $W(m)$ is still symmetric around $m = N/2$, but now the two peak positions shift to $m \simeq N/2 \pm \frac{1}{2}d_{LR}/\sigma$ for the same reason as for this shape, the entropic forces are balanced at the left side of the left pore and at the right side of the right pore. Similar to what is observed for the single nanopore, $\tilde{W}(m)$ rises roughly linearly for $m < N/2 - \frac{1}{2}d_{LR}/\sigma$, until peaks at $m \simeq N/2 - \frac{1}{2}d_{LR}/\sigma$. It then decreases to a minimum at $m = N/2$, rises, and peaks again at $m = N/2 + \frac{1}{2}d_{LR}, /\sigma$ and then goes down almost linearly, as shown in Fig. 3(a). The two noticeable kinks at 0.5 ± 0.3, where a change of slope occurs, are when the monomers have exited either of the pores and subject to a net bias force. It is also worth noticing that $W(m)$ has a local minimum

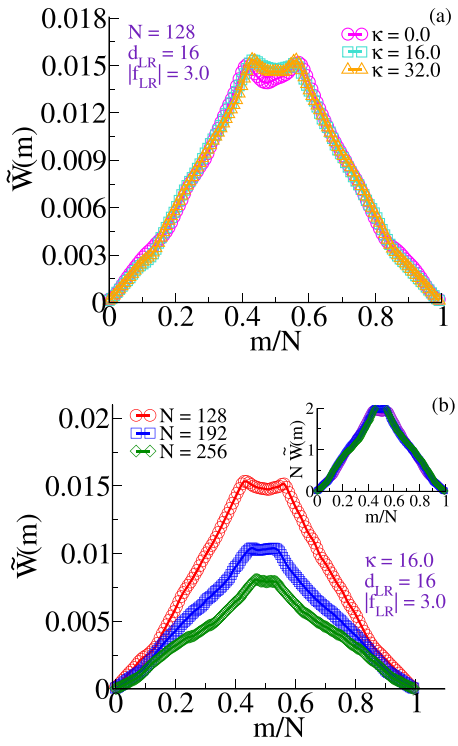

FIG. 3. (a) Normalized dwell time distribution $\tilde{W}(m)$ as a function of reduced monomer index m/N for $N = 128$ for $\kappa = 0$ (magenta circles), 16 (teal squares), and 32 (orange diamonds) respectively. (b) $\tilde{W}(m)$ shows the chain length dependence ($N = 128$, 192, and 256 of $W(m)$ for $\kappa = 16.0$. The inset confirms that qualitative behavior remains uniform for $N\tilde{W}(m)$ with the reduced monomer index for different chain lengths.

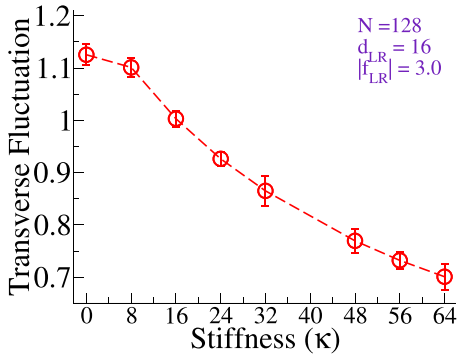

FIG. 4. Transverse fluctuation shows a steady decrease with increasing chain stiffness k.

at the midpoint of the chain $m = N/2$. The monomer with index $m = N/2$ lowers the free energy by staying equidistant from the two pores, which decreases its residence time at each pore. This explains the shape of Fig. 3(a). We further observe that $\tilde{W}(m)$ is almost insensitive to the chain stiffness. An increase in the chain stiffness causes the translocation time $\langle\tau\rangle$ to increase[16] (shown at the inset), and the collapse of $\langle\tilde{W}(m)\rangle$ for different stiffness onto the same master curve implies that $\langle\tilde{W}(m)\rangle$ for each m increases proportionally with the translocation time. In addition, Fig. 3(b) confirms that $\langle\tilde{W}(m)\rangle$ scales uniformly with chain lengths, and the inset shows an excellent data collapse for $N\langle\tilde{W}(m)\rangle$ against the reduced monomer index.

Interestingly, we observe that $\tilde{W}(m)$ is also insensitive to the rms transverse fluctuation $\sqrt{\langle l_\perp^2\rangle}$ of the segment in between the pores that decreases monotonically with increasing chain stiffness (Fig. 4). In the simulation, we measure the rms transverse fluctuation as follows:

$$\sqrt{\langle l_\perp^2\rangle} = \sqrt{\frac{1}{m_{pore}}\sum_{i_{pore}=1}^{m_{pore}}\left(y_i^2 + z_i^2\right)}, \tag{9}$$

where y_i and z_i are the vertical distances of the i-th monomer with respect to the direction $\hat{x}$ from the left pore and the right pore and m_{pore} are the number of monomers in between the two pores. This decrease in $\sqrt{\langle l_\perp^2\rangle}$ is a generic feature for the chain segment under tension. We have explained it elsewhere by mapping the translocation problem to that of a *flexible-stiff-flexible* triblock copolymer.[12] Combining the results from Figs. 2–4, we conclude that despite variations in chain stiffness and transverse fluctuations for the segment in between the pores, the normalized dwell time distributions $\tilde{W}(m)$ collapse onto the same master curve. This is an important result that can be used to extrapolate the experimental data obtained for one contour length and stiffness to different contour lengths and chain stiffness without running a separate experiment.

C. The tug-of-war and the escape

A central question in polymer translocation is how long does it take for the chain to escape from one side to the other. This has been

Published under license by AIP Publishing

described in terms of a translocation exponent α, which determines the power law dependence of the mean translocation time $\langle\tau\rangle$ on the chain length N,

$$\langle\tau\rangle = AN^{\alpha}. \tag{10}$$

We already saw that the dwell time is very similar to that of a single nanopore, and we expect that for $d_{LR} \ll L$, the escape problem in a double nanopore will also be described by a similar power law dependence of $\langle\tau\rangle$ on N. In this limit, the contribution of the segment in between the two nanopores becomes insignificant; thus, one expects that the exponent α will be the same as that of a single nanopore. We have obtained the escape time $\langle\tau\rangle$ from the BD simulation for the symmetrically placed and cocaptured polymer in between two nanopores for $\vec{f}_L + \vec{f}_R = 0$. Due to the symmetric arrangement, the case escape occurs equally through the left pore and the right pore. By monitoring 2000 independent runs, we checked that translocation occurs with equal probability in either direction.

1. Decoupling the chain stiffness

First, we discuss how the escape problem for the fully flexible chain can be generalized for a stiff chain by calculating the stand-alone stiffness factor. The escape problem through an idealized nanopore in a thin membrane has been studied theoretically by various authors.[26–29] For a fully flexible chain, it was proposed[27,29] that $\alpha = 1 + 2\nu$ so that the average translocation time for the unbiased translocation scales with the chain length as $\langle\tau_0\rangle = AN^{1+2\nu}$. This follows assuming the quasi-equilibrium condition so that the gyration radius, $\langle R_g\rangle \sim N^{\nu}$, is the same as that of the bulk and that in the absence of the hydrodynamic effects, the diffusion constant of the center of mass of the chain is $D \sim 1/N$. Thus, the translocation time $\langle\tau\rangle$ to travel a distance of the order of $\langle R_g\rangle$ can be estimated by substituting

$$\langle R_g^2\rangle \sim N^{2\nu} \tag{11}$$

in the diffusion equation $\langle R_g^2\rangle \sim D\langle\tau\rangle$, which results in

$$\langle\tau_0\rangle \sim \langle R_g^2\rangle/D = AN^{1+2\nu}. \tag{12}$$

Thus, the translocation time in this picture scales as the Rouse relaxation time.[25]

Equation (12) for a fully flexible chain can be generalized for a semiflexible chain using the generalized Flory theory due to the work of Nakanishi[30] and Schaefer, Joanny, and, Pincus,[31] which incorporates the persistence length ℓ_p into the Flory equation (11) as follows:

$$\sqrt{\langle R_g^2\rangle} \sim \ell_p^{1/(D+2)} N^{\nu} \tag{13}$$

in D physical dimensions. Previously, we have shown that in two dimensions (2D), Eq. (13) holds for $L/\ell_p > 1$.[17] Hence, for the unbiased translocation, the generalization for the translocation time $\langle\tau_{\ell_p}\rangle$ for a semi-flexible chain of persistence length l_p is

$$\langle\tau_{\ell_p}\rangle = A\ell_p^{\frac{2}{D+2}} N^{1+2\nu} = \langle\tau_0\rangle \ell_p^{\frac{2}{D+2}}. \tag{14}$$

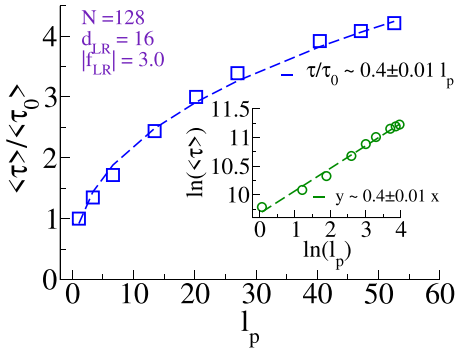

FIG. 5. $\langle\tau_{\ell_p}\rangle/\langle\tau_0\rangle$ as a function of ℓ_p (blue squares). The dotted line is a power law fit ($\langle\tau_{\ell_p}\rangle/\langle\tau_0\rangle \sim \ell_p^{0.4}$) through the points validating Eq. (14). The inset shows the same (green circles) on a log–log scale. The straight line is a linear fit with slope 0.40 ± 0.01.

In making generalization of Eq. (12) to Eq. (14), we assumed that the amplitude factor A remains the same. In other words, we have decoupled that stiffness factor from the intrinsic translocation time of a fully flexible chain, an assumption is not fully justified *a priori*. However, we observe that this works reasonably well for the escape problem that we have studied here. Slater[33] and Panja[34] have suggested an alternative expression for $\langle\tau_0\rangle$ based on the memory effect to Eq. (12) where the exponent is $\alpha = 2 + \nu$ so that $\langle\tau_0\rangle \sim N^{2+\nu}$. If we assume that the stiffness factor $\ell_p^{2/D+2}$ decouples from the solvent factor, then instead of Eq. (14), one gets $\langle\tilde{\tau}_{\ell_p}\rangle = \tilde{A}\ell_p^{\frac{2}{D+2}} N^{2+\nu} = \langle\tilde{\tau}_0\rangle \ell_p^{2/D+2}$. Here, $\langle\tilde{\tau}_0\rangle = \tilde{A}N^{2+\nu}$. We assume that the stiffness factor $\ell_p^{2/D+2}$ enters in to this equation the same way as in Eq. (14) irrespective of the mechanism of $\langle\tilde{\tau}_0\rangle$. Figure 5 verifies this decoupling of the stiffness factor from the intrinsic translocation time $\langle\tau_0\rangle$ for a fully flexible chain. In 3D, the factor is $\ell_p^{2/D+2} = \ell_p^{0.4}$. A plot of $\langle\tau_{\ell_p}\rangle/\langle\tau_0\rangle$ as a function of the chain persistence length ℓ_p validates the prefactor $\ell_p^{2/D+2} = \ell_p^{0.4}$ in Eq. (14). In Sec. III C 2, we explore the chain length dependence of $\langle\tau_0\rangle \sim N^{\alpha}$ in the double nanopore system.

2. The translocation exponent

Having theoretically justified and validated by simulation Eq. (14), we now use the simulation data for different contour and persistence lengths to study the exponent α [Eq. (10)] and discuss the result in the context of a single nanopore escape problem. The polymer escape problem has been studied by several authors in the past, making its connection to the translocation problem.[27–29,32,33,36] One would like to distinguish between translocation and escape in this context. Typically, in a translocation problem, the entire chain crosses from the *cis* side of the pore to the *trans* side. For the case of driven translocation, simulation studies are also carried out by placing the first monomer either at the center of the pore or slightly shifted at the *trans* side.[19,20] For the unbiased case, this will be prohibitively large, as the polymer has to cross a huge barrier. In order to circumvent this problem, Chuang, Kantor, and Kardar (CKK) put an artificial constraint that once a monomer is on the *cis* side, it cannot go back to the

Published under license by AIP Publishing

trans side.[29] With this constraint, their numerical calculation converged on the translocation time $\langle\tau\rangle = AN^{1+2\nu}$. CKK further argued that the prefactor is larger compared to the unconstrained case to account for the slower diffusion due to the constraint imposed by the nanopore and the wall and concluded that for the unbiased case, the translocation exponent is the same as the as that of the relaxation process.

Dubbeldam *et al.*[35] mapped the escape problem in the one-dimensional anomalous diffusion problem in terms of the reaction coordinate and predicted the anomalous exponent $\alpha' = 2/(2\nu + 2 + \gamma_1) = 0.801(3d)$ by introducing the surface exponent term $\gamma_1 = 0.68(3d)$. Dubbeldam *et al.* set up MC simulation with a directional constraint on polymer movement and showed $\langle\tau_0\rangle \propto N^{2/\alpha'} = N^{2.496}$, which agrees with their theoretical framework. de Haan and Slater[33] incorporated memory effects during unbiased-translocation and asymptotically estimated $\langle\tau_0\rangle \sim N^{2.516}$ for a very long polymer.

Luo *et al.* revisited the same problem in two dimensions and studied polymer escape through a single nanopore using the bond-fluctuation model.[36] Their initial condition is the same as ours, namely, to release the polymer from the peak of the entropic barrier and let it diffuse down the entropic valley. They observed that for the escape problem in 2D ($\nu = 0.75$), $\langle\tau\rangle \sim N^{2.5}$, confirming that the escape problem and the translocation problem have the same (relaxation) exponent $1 + 2\nu$.

We studied the same problem albeit in the context of a double nanopore and having the DNA in a tug-of-war with two equal and opposite forces so that the net force is zero. Specifically, we studied the variation of the exponent α, when one increases the chain persistence length from $\ell_p < d_{LR}$ to $\ell_p > d_{LR}$. The logarithmic plots in Fig. 6(b) ($\ell_p < d_{LR}$) and Fig. 7(b) $\ell_p > d_{LR}$ show a systematic increase in slope (α) from 2.37 to 2.52 as expected due to the stiffness factor $\ell_p^{0.4}$ in Eq. (14) as ℓ_p is increased from 4–32. However, Figs. 6(c) and 7(c) show plots of $\tau_{\ell_p}/\ell_p^{0.4} = \langle\tau_0\rangle \sim N^{\alpha}$ [see Eq. (14)] where the data for different ℓ_p collapse on to the same straight line. We obtain $\alpha = 2.4 \pm 0.05$ for $\kappa = 4$ and 8 ($\ell_p < d_{lR}$)

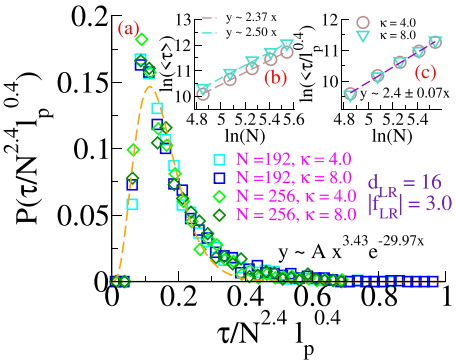

FIG. 6. (a) Histograms of normalized escape time $\tau/N^{2.4}\ell_p^{0.4}$ for chain length $N = 192$ (cyan and blue squares for $\kappa = 4.0$ and 8.0) and for $N = 256$ (light and dark green diamonds for $\kappa = 4.0$ and 8.0), respectively, show data collapse. (b) $\langle\tau\rangle$ as a function of N (log scale) shows slopes 2.37 and 2.50 for $\kappa = 4.0$ and 8.0, respectively. (c) The renormalized $\langle\tau\rangle/\ell_p^{0.4}$ as a function of N (log scale), which shows collapse of both the curves with slope $\alpha = 2.40 \pm 0.07$ consistent with (a).

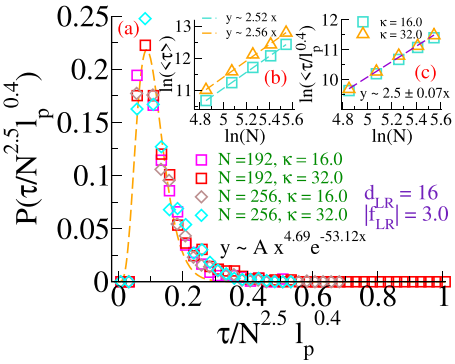

FIG. 7. (a) Histograms of normalized escape time $\tau/N^{2.5}\ell_p^{0.4}$ for chain length $N = 192$ (magenta and red squares for $\kappa = 16.0$ and 32.0) and for $N = 256$ (brown and cyan diamonds for $\kappa = 16.0$ and 32.0), respectively, show data collapse. (b) $\langle\tau\rangle$ as a function of N (log scale) shows slopes 2.52 and 2.56 for $\kappa = 16.0$ and 32.0, respectively. (c) The renormalized $\langle\tau\rangle/\ell_p^{0.4}$ as a function of N (log scale), which shows collapse of both the curves with slope $\alpha = 2.50 \pm 0.07$ consistent with (a).

and $\alpha = 2.5 \pm 0.04$ for $\kappa = 16$ and 32 ($\ell_p > d_{lR}$), respectively. This is further ensured from the data collapse in Figs. 6(a) and 7(a). We further observe that as in the case of a double nanopore translocation problem, the shape of the histogram can be fitted with $P(x) \sim x^{\alpha}\exp(-\beta x)$ with the maximum located at α/β. We verify that $\int_0^{\infty} x.P(x)dx$ returns back the mean translocation time $\langle\tau\rangle$. Thus, for the double nanopore translocation, we observe that the translocation exponent $\alpha > 1 + 2\nu$ and α increases with increasing stiffness. Since we have decoupled the intrinsic chain stiffness, this slow down of the translocation process is likely due to additional constraints imposed by the double nanopore.

IV. SUMMARY AND CONCLUDING REMARKS

We have studied the polymer escape problem in a double nanopore system in a tug-of-war situation where the distance between the pores is much smaller than the chain contour length for several chain persistence lengths. The problem bears similarities with the much studied problem of escape of a fully flexible chain through a single nanopore. However, because of the presence of the two equal and opposite forces, our simulation studies reveal additional intriguing features. First, during the escape process, the chain segments in the region between the pores acquires increased stiffness, which becomes more prominent for a fully flexible chain but also noticeable for stiffer chains. In contrast, the scaled dwell time distributions for different chain stiffness collapse onto the same master curve, indicating that an increased chain stiffness introduces a global shift in the dwell time distribution of the individual monomers with respect to the total translocation time.

We proposed a generalization of the chain length dependence of the escape problem for semi-flexible chains [Eq. (14)]. Our simulation data establish an important aspect of the escape problem that the stiffness factor arising from the generalization of the Flory theory [Eq. (13)] decouples from the escape time of a fully flexible chain, and thus, to a first approximation, the theories developed for a fully

Published under license by AIP Publishing

flexible chain can be applied here leading to Eq. (14). Our simulation studies validate that for a given contour length, the escape time increases as a power law $\ell_p^{2/D+2}$. For the unbiased translocation, the chain conformations are in quasi-equilibrium, and hence, Eq. (13) is valid. However, we observe from the plot of $\langle\tau\rangle/\ell_p^{2/D+2} = \langle\tau_0\rangle = AN^{\alpha}$ [Insets of Figs. 6(b) and 7(b)] that the translocation exponent α depends on the chain stiffness and increases from 2.4 ± 0.01 to 2.5 ± 0.01. This arises due to the additional constraint imposed by the two pores and the system to develop characteristics of a reptation,[25] which is intrinsically a slower process than diffusion.

It is also worth noting that, in general, nanopore experiments are conducted in electrolyte solutions that span orders of magnitude (mM-M range). This does have an impact on the persistence length. The scaling relation can be used to predict the experimental outcome when one varies the electrolyte solution. Second, experimentally, no two drilled nanopores are identical (for example, in Ref. 10, the diameters of the two nanopores were 25 nm and 27 nm, and the pore-to-pore distance is 610 nm). However, unlike Ref. 1, where the pore diameters were made to be different (10 nm and 16 nm), in Ref. 10, it is more desirable to have the difference as small as possible to have the same time of flight from the left to the right pore and vice versa the same for the same oscillating differential bias. Thus, it will be worthwhile to design simulation with slightly different pore diameters to estimate the asymmetry in time of flight from left to right and vice versa. We believe that these results and discussions will be useful for future double nanopore experiments.

ACKNOWLEDGMENTS

The authors acknowledge computing resources under the auspices of UCF's high performance computing cluster STOKES where all the computations were done and thank both the referees for their constructive comments on the earlier version of this manuscript.

DATA AVAILABILITY

The data that support the findings of this study are available from the corresponding author upon reasonable request.

REFERENCES

[1] S. Pud, S.-H. Chao, M. Belkin, D. Verschueren, T. Huijben, C. van Engelenburg, C. Dekker, and A. Aksimentiev, Nano Lett. **16**, 8021 (2016).
[2] J. J. Kasianowicz, E. Brandin, D. Branton, and D. W. Deamer, Proc. Natl. Acad. Sci. U. S. A. **93**, 13770 (1996).
[3] A. Meller, L. Nivon, E. Brandin, J. Golovchenko, and D. Branton, Proc. Natl. Acad. Sci. U. S. A. **97**, 1079 (2000).
[4] A. Meller, L. Nivon, and D. Branton, Phys. Rev. Lett. **86**, 3435 (2001).
[5] A. Meller and D. Branton, Electrophoresis **23**, 2583 (2002).
[6] P. Cadinu *et al.*, Nano Lett. **17**, 6376 (2017).
[7] P. Cadinu *et al.*, Nano Lett. **18**, 2738 (2018).
[8] J.-W. Yeh, Nano Lett. **12**, 1597 (2012).
[9] Y. Zhang, X. Liu, Y. Zhao, J.-K. Yu, W. Reisner, and W. B. Dunbar, Small **14**, 1801890 (2018); X. Liu, Y. Zhang, R. Nagel, W. Reisner, and W. B. Dunbar, *ibid.* **15**, 1901704 (2019).
[10] X. Liu, P. Zimny, Y. Zhang, A. Rana, R. Nagel, W. Reisner, and W. B. Dunbar, Small **16**, 1905379 (2019).
[11] For recent reviews in the field please see M. Muthukumar, *Polymer Translocation* (CRC Press, Boca Raton, 2011); A. Milchev, J. Phys.: Condens. Matter **23**, 103101 (2011); D. Panja, J. Stat. Mech. **2010**, P06011; V. V. Palyulin, T. Ala-Nissila, and R. Metzler, Soft Matter **10**, 9016 (2014); B. M. Venkatesan and R. Bashir, Nat. Nanotechnol. **6**, 615 (2011).
[12] A. Bhattacharya and S. Seth, Phys. Rev. E **101**, 052407 (2020).
[13] T. Ahmed *et al.*, Nanotechnology **25**, 125705 (2014).
[14] G. S. Grest and K. Kremer, Phys. Rev. A **33**, 3628(R) (1986).
[15] A. D. Sokal, in *Monte Carlo and Molecular Dynamics Simulations in Polymer Science*, edited by K. Binder (Oxford University Press, New York, 1995), Chap. 2.
[16] R. Adhikari and A. Bhattacharya, J. Chem. Phys. **138**, 204909 (2013).
[17] A. Huang, A. Bhattacharya, and K. Binder, J. Chem. Phys. **140**, 214902 (2014).
[18] A. Huang, H.-P. Hsu, A. Bhattacharya, and K. Binder, J. Chem. Phys. **143**, 243102 (2015).
[19] A. Bhattacharya and K. Binder, Phys. Rev. E **81**, 041804 (2010).
[20] A. Bhattacharya, W. H. Morrison, K. Luo, T. Ala-Nissila, S.-C. Ying, A. Milchev, and K. Binder, Eur. Phys. J. E **29**, 423 (2009).
[21] K. Luo, T. Ala-Nissila, S.-C. Ying, and A. Bhattacharya, Phys. Rev. Lett. **99**, 148102 (2007); **100**, 058101 (2008).
[22] L. D. Landau and E. M. Lifshitz, *Statistical Physics: Part 1*, 3rd ed. (Pergamon Press, 1980).
[23] W. F. van Gunsteren and H. J. C. Berendsen, Mol. Phys. **45**, 637 (1982).
[24] M. P. Allen and D. J. Tildesley, *Computer Simulation of Liquids*, 2nd ed. (Oxford University Press, 2017).
[25] M. Rubinstein and R. H. Colby, *Polymer Physics* (Oxford University Press, 2003).
[26] K. Luo *et al.*, Phys. Rev. E **78**, 050901(R) (2008).
[27] M. Muthukumar, J. Chem. Phys. **111**, 10371 (1999).
[28] W. Sung and P. J. Park, Phys. Rev. Lett. **77**, 783 (1996).
[29] J. Chuang, Y. Kantor, and M. Kardar, Phys. Rev. E **65**, 011802 (2001).
[30] H. Nakanishi, J. Phys. **48**, 979 (1987); J. Moon and H. Nakanishi, Phys. Rev. A **44**, 6427 (1991).
[31] D. W. Schaefer, J. F. Joanny, and P. Pincus, Macromolecules **13**, 1280 (1980).
[32] M. G. Gauthier and G. W. Slater, Phys. Rev. E **79**, 021802 (2009).
[33] H. W. de Haan and G. W. Slater, J. Chem. Phys. **136**, 154903 (2012).
[34] D. Panja, G. T. Barkema, and R. C. Ball, J. Phys.: Condens. Matter **19**, 432202 (2007).
[35] J. L. A. Dubbeldam, A. Milchev, V. G. Rostiashvili, and T. A. Vilgis, Phys. Rev. E **76**, 010801(R) (2007).
[36] K. Luo *et al.*, J. Chem. Phys. **124**, 034714 (2006).

Published under license by AIP Publishing